

# Synthesis and Catalytic Properties of Nickel–Silica Composite Hollow Nanospheres

Pu Jin,<sup>†</sup> Qianwang Chen,<sup>\*,†</sup> Liqing Hao,<sup>‡</sup> Ruifen Tian,<sup>‡</sup> Lixin Zhang,<sup>†</sup> and Lin Wang<sup>†</sup>

Structure Research Laboratory and Department of Materials Science and Engineering, and Department of Chemical Physics, University of Science and Technology of China, Hefei 230026, China

Received: January 16, 2004; In Final Form: March 14, 2004

A coating process was applied to prepare nickel–silica composite hollow nanospheres (650 nm) with controllable shell thickness. The nanospheres were characterized through X-ray diffraction, transmission electron microscopy, and field emission scanning electron microscopy. This material with large BET surface area (288 m<sup>2</sup>/g) exhibits good catalytic activity and high selectivity in acetone hydrogenation reaction, showing the potential application as a catalyst in industry.

## Introduction

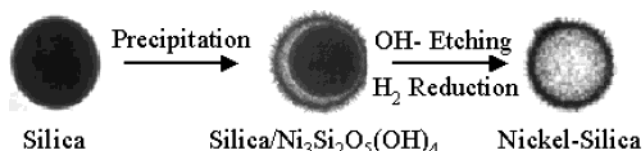
Recently, monodisperse nanospheres, core–shell nanostructures, and hollow nanospheres with uniform physical and chemical properties have received much attention because they have potential applications, such as photonic materials and microchip reactors.<sup>1–6</sup> The common route for preparing hollow nanospheres is to coat nanocrystals on the template spheres followed by removing the templates through etching or calcinations.<sup>7</sup> Colvin et al. had successfully developed such a route to produce macroporous metals such as three-dimensional nickel films with pore diameters between 200 and 1000 nm. The porous nickel formed in that way is over 70% air—resulting with large surface area and sturdy structure that was suggested to be useful in wide fields ranging from sensors to catalysis.<sup>8,9</sup> It is also well-known that the shape, size, and utility or properties are inextricably linked. The architectures designed and fabricated from appropriate nanoscale building blocks, including the use of void space, show some new opportunities for improving the performance of the catalyst.<sup>10</sup>

In this paper, we reported a process for synthesizing nickel–silica composite hollow nanospheres with needlelike nickel particles embedded in a silica shell. The mesoporous and macroporous structures present in these spheres give the potential applications in catalyst or an active carrier for catalyst. This type of catalytic architecture differs from standard impregnated catalysts that are described as a metal “flea” riding on oxide “boulder” in some literature.<sup>10–12</sup> In our process the amount of metal particles loaded on the silica carriers is much larger.

## Experimental Section

All the reagents used in this investigation were analytical grade and used without further purification. The monodisperse silica nanospheres were prepared according to the process developed by Stöber et al.<sup>13</sup> This method comprises two steps: the hydrolysis and polycondensation of tetraethoxysilane (TEOS) under alkaline conditions in ethanol. The starting reagents contained 6 mL of TEOS, 62 mL of ethanol, and 12 mL of

## SCHEME 1: Schematic Illustration for the Preparation of Nickel–Silica Composite Hollow Nanospheres<sup>a</sup>



<sup>a</sup> The graphs are actual TEM images of the samples obtained at each step.

28% ammonia as catalyst. The mixture was stirred mildly for 1 h, and the product weighed about 1.2 g after washing and drying.

The whole synthesis process is illustrated briefly in Scheme 1. First, 1.2 g of SiO<sub>2</sub> spheres were dispersed in 100 mL of solution containing 0.15 g of Ni(NO<sub>3</sub>)<sub>2</sub>·6H<sub>2</sub>O and 0.3 g of CO-(NH<sub>2</sub>)<sub>2</sub>. The suspension was stirred mildly at a constant temperature of 95 °C for 4 h to precipitate completely, and the system was about pH 8 at the end of the reaction. The process for preparing uniform shells on silica cores by homogeneous precipitation of slowly decomposing urea in nickel nitrate solution was repeated several times,<sup>12</sup> which controls the thickness of the uniform layers. By immersing the core–shell powder in 200 mL of 0.5 mol/L NaOH, the silica cores were dissolved by alkaline and the remainder shells were washed by distilled water until the pH of filtrate was lower than pH 7.0. After being dried in a vacuum stove, these powders were reduced in H<sub>2</sub> current (40 mL min<sup>−1</sup>) at 450 °C for 1 h in the fixed-bed reactor and the products were kept in N<sub>2</sub> current for 10 h after the temperature decreased to 60 °C, which would prevent most of the product from forming oxide when exposed to air.

The chemical composition of the hollow capsules was analyzed by X-ray fluorescence spectrum and dimethyl glyoxime gravimetric analysis. The phases of the mediate and ultimate product were also determined by X-ray diffraction (XRD). The morphology and microstructure of the hollow spheres were observed through transmission electron microscopy (TEM) and scanning electron microscopy (SEM). BET surface area was obtained by N<sub>2</sub> adsorption/desorption isotherm data, while the hydrogen adsorption on the samples was investigated by pressure–composition–temperature (PCT) measurement at a temperature of 25 °C and under hydrogen pressure ranging from 0.01 to 40 atm, which is the normal measurement for hydrogen storage.<sup>14</sup>

\* To whom correspondence should be addressed. E-mail: cqw@ustc.edu.cn.

<sup>†</sup> Structure Research Laboratory and Department of Materials Science and Engineering.

<sup>‡</sup> Department of Chemical Physics.

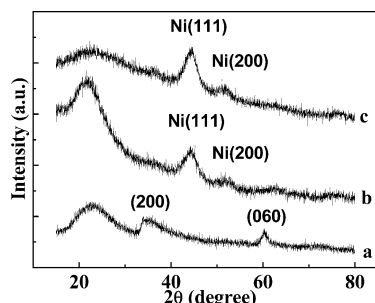


**Figure 1.** XRD patterns of different nanospheres: (a) freshly coated silica spheres, showing the formation of  $\text{Ni}_3\text{Si}_2\text{O}_5(\text{OH})_4$ ; (b) silica/nickel core-shell structure, reduction at 550 °C before removing silica, showing the presence of a large amount of silica with a broad diffraction band peaking at 26.2°; (c) nickel-silica composite hollow spheres, with reduction at 450 °C after removing silica, showing the decrease of the amount of silica.

The catalytic activity of this material and the activity as carrier for noble metal catalysts were studied by acetone hydrogenation reaction at 373, 423, and 473 K.<sup>16</sup> A 1.0 wt % amount of Pd was precipitated on the pure silica nanospheres and the composite hollow spheres, respectively. At atmospheric pressure, 0.30 g of catalysts was reduced according to the above method but without  $\text{N}_2$  treatment. The packed bed reactor was a cylindrical tube with the diameter of 1 cm, and the length of the part where the catalyst (0.30 g) lied was nearly 2.5 cm. Then the hydrogenation reactions were carried out directly without taking the catalysts out of the reactor to keep the clean surface of the catalysts. When at reaction, the experiments were carried out in the current of the mixture of acetone and  $\text{H}_2$  instead of pure  $\text{H}_2$ . The volume ratio of acetone to  $\text{H}_2$  was about 1:4, and the  $\text{H}_2$  current was 120 mL  $\text{min}^{-1}$ . The reaction time lasted for 70 min if the acetone was 10 mL. The products were collected at 0 °C and analyzed by GC-MS.

## Results and Discussion

Through the hydrolysis and condensation of TEOS under alkaline condition, monodisperse silica nanospheres with an average diameter of about 400 nm were obtained. These silica nanospheres will be utilized as cores, the templates, to form uniform shells by homogeneous precipitation of slowly decomposing urea in nickel nitrate solution. The diffraction peak from amorphous  $\text{SiO}_2$  was around  $2\theta = 26.2^\circ$ , which can be clearly observed in patterns a and b of Figure 1, but was not so obvious in c because the silica cores were removed by alkaline solution. In pattern a, the peaks for (200) and (060) are aroused from monoclinic nickel hydrosilicate, a thermal stable substance at 500 °C.

It is reported that only nickel hydrosilicate would be obtained on the surface of silica spheres due to the interactions between silica spheres and nickel particles, and this effect was more obvious at high temperatures.<sup>12</sup> This shell could not be reduced completely even at 550 °C, though increasing temperature might favor this process.<sup>12</sup> To confirm the temperature of heat treatment, nickel hydroxide without silica was synthesized by the same method. TG analysis shows there is an obvious weight loss at 320 °C, which might correspond to the decomposition of hydroxide. The decomposed product was face-centered cubic NiO. However, because nickel hydrosilicate was formed, this transformation in the core-shell structure was not noticed even though the powder was calcined at 500 °C for 5 h. The X-ray diffraction patterns in Figure 1 a,b show that  $\text{Ni}_3\text{Si}_2\text{O}_5(\text{OH})_4$  and metallic nickel formed on the surface of silica nanospheres after coating and further reducing, respectively. It was also found

**TABLE 1: X-ray Fluorescence Spectrum and X-ray Photoelectron Spectroscopy Quantitative Analysis Results of Nickel-Silica Composite Hollow Spheres**

(a) X-ray Fluorescence Spectroscopy			
element	at. %	element	at. %
Ni	57.9	K	0.5
Si	37.4	Ca	0.4
Na	2.3	Fe	0.3
Al	1.0	S	0.2

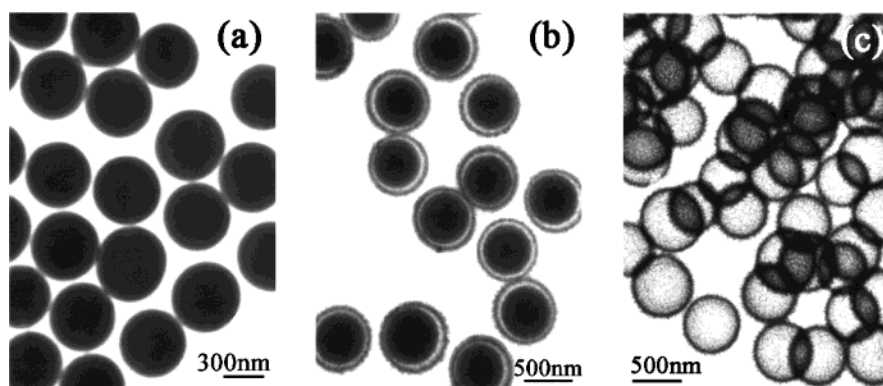
  

(b) X-ray Photoelectron Spectroscopy			
peak ID	at. %	peak ID	at. %
C 1s	8.53	Ni 2p3	16.61
O 1s	56.21	Si 2p	18.65

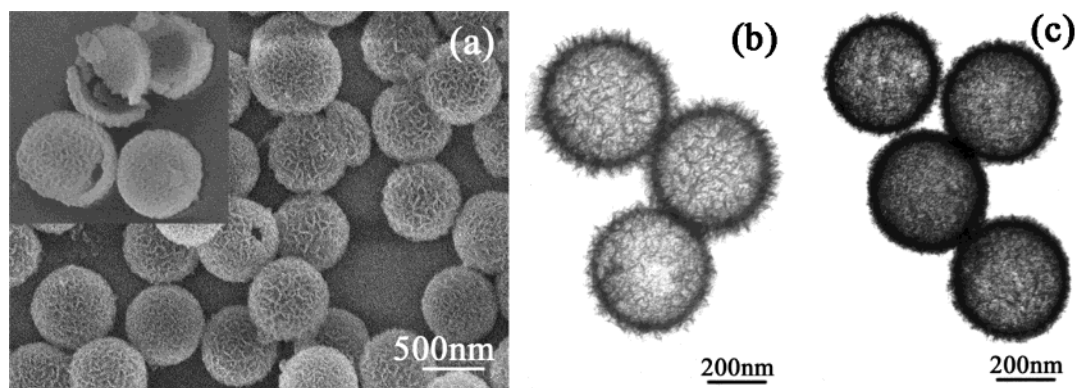
that the newly prepared silica would interact with the nickel more easily than those after aging for several days. To decrease this strong interaction, the silica cores were removed before reduction, which made the shells more easily to be reduced even at 450 °C. As shown in Figure 1c, the XRD pattern of the sample depicts a significant decrease in the intensity of the diffraction peak at 26.2°, indicating this process easily removes silica cores. According to the Scherrer's equation, the particle size of nickel crystallites calculating from the peak Ni(111) is about 12.8 nm. The X-ray fluorescence spectrum data show that the atomic ratio of Ni to Si is 57.9 to 37.4. Furthermore, from the XPS peaks of Ni 2p3 and Si 2p, it could be also known that Ni to Si is 16.61 to 18.65 on the surface of the shell. The impurities and its contents were shown in Table 1a, which might be induced in experiment or analysis process. The great amount of C and O in XPS data (Table 1b) might be brought by the  $\text{CO}_2$  and  $\text{O}_2$  adsorbing on the active surface of nickel-silica composite hollow nanospheres. All these data, especial those from dimethyl glyoxime gravimetric analysis, prove that the weight of nickel is more than 40% in the final product. It is therefore called the product nickel-silica composite hollow nanospheres due to certain amounts of silica still exist on the inner surface of the hollow spheres as matrixes for Ni nanoparticles to form shells.

After the coating process, the surface morphology changed a lot. Figure 2a shows the TEM image of the bare silica nanospheres with smooth surface and spherical shape. Figure 2b shows clearly the core-shell structure of silica/ $\text{Ni}_3\text{Si}_2\text{O}_5(\text{OH})_4$  with the shell thickness about 40 nm; the thickness could be controlled by the times of coating, and each coating might increase the thickness for 5 nm. The shells consist of needlelike particles as revealed by TEM image (Figure 3b). Because of the formation of a new compound of  $\text{Ni}_3\text{Si}_2\text{O}_5(\text{OH})_4$  and the needlelike structure on the core-shell interface, the shells began to separate from the cores with increasing thickness of the shells. The TEM image reveals that the sheetlike phase did not contact with the silica core closely (Figure 2b), which might cause this separation. Just because of this separation, it has much probability to remove the core without destroying the shell. To keep the spherical shape of the shell, the concentration of strong base should be carefully controlled to avoid distortion of the shell. Because of the support of the core, the shell did not collapse when these powders were dispersed by ultrasound. After reduction the morphology of the shells (Figure 3b,c) did not change when compared to those before the reaction (Figure 2b).

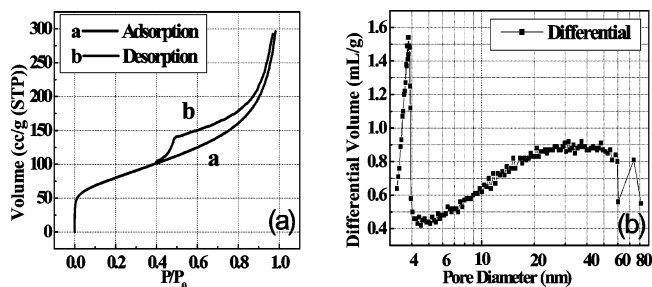
In Figure 2c, the bright areas inside the spheres indicate that the  $\text{SiO}_2$  cores were removed after treatment in alkaline solution, while the surface morphology did not change significantly. The SEM image reveals that the shells are composed of nanoparticles with an average size of 15 nm integrating closely to form an uniform layer (Figure 3a), and the broken shells in the inset of



**Figure 2.** TEM images of (a) bare silica spheres and (b) silica/ $\text{Ni}_3\text{Si}_2\text{O}_5(\text{OH})_4$  core-shell structures; (c)  $\text{Ni}_3\text{Si}_2\text{O}_5(\text{OH})_4$  hollow spheres with an average size of 650 nm. Nickel–silica composite hollow nanospheres with shell thickness about 40 nm.



**Figure 3.** SEM image of (a)  $\text{Ni}_3\text{Si}_2\text{O}_5(\text{OH})_4$  hollow nanospheres. Inset shows broken hollow nanospheres. TEM images of nickel–silica hollow nanospheres prepared by reduction after removing silica cores (b) and removing silica cores after reduction (c).



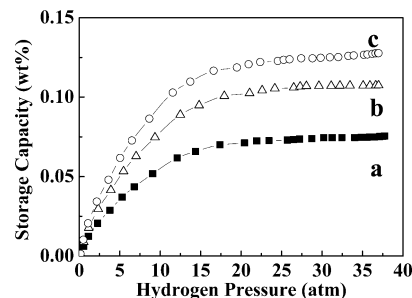
**Figure 4.**  $\text{N}_2$  adsorption/desorption isotherm (a) and pore diameter distribution (b) of nickel–silica composite hollow spheres.

Figure 3a also confirm that the spheres are hollow. The SEM image also shows that these layers are of porous structure (Figure 3a), which is much different from the smooth interface of the bare silica nanospheres. It is expected that this porous structure would be favorable for the transportation of  $\text{H}_2$  and  $\text{H}_2\text{O}$  during reduction.

It might be due to magnetic interaction between nickel nanoparticles; most of the nickel–silica layers did not break up after heating and cooling.

The surfaces of the nanoshells prepared by removing the cores after the reduction process were smoother than those prepared by reduction of hollow nickel hydrosilicate. Such a surface change did not occur in the latter process so that the porous surface was reserved. To reduce the shell more completely and keep the porous surface that is believed to possess a larger surface area, the latter approach is suitable.

The shape of the  $\text{N}_2$  adsorption/desorption isotherm (Figure 4) of nickel–silica hollow nanospheres further reveals the characteristic of their porosity. The BET surface area is about  $288 \text{ m}^2 \text{ g}^{-1}$ , which is larger than that of Raney Ni ( $95 \text{ m}^2 \text{ g}^{-1}$ )<sup>15</sup>



**Figure 5.** PCT measurement of samples: (a) normal nickel particles prepared by the same coprecipitation and reduction process without silica cores; (b) nickel–silica composite hollow nanospheres without  $\text{N}_2$  treatment; (c) nickel–silica composite hollow nanospheres being treated with  $\text{N}_2$  for 12 h after reduction.

and corresponds to that of other catalyst carriers such as  $\text{Al}_2\text{O}_3$  and  $\text{SiO}_2$ . The pore volume of the sample is  $0.396 \text{ mL g}^{-1}$ , and the mean pore diameter is 19.53 nm. A majority of the pores have a diameter less than 4 nm, which might exist in silica matrix; other pores with sizes from 10 to 60 nm might come from the aggregates of Ni nanoparticles.

The PCT measurement results (Figure 5) show that the normal nickel particles have the lowest  $\text{H}_2$  adsorption capacity under the same condition, while the nickel–silica composite hollow spheres display better  $\text{H}_2$  adsorption properties. The difference between the latter two samples is that sample b was taken out of the reactor without the  $\text{N}_2$  treatment after cooling to room temperature with part of the nickel being oxidized in air. The  $\text{N}_2$  treatment at room temperature could remove the  $\text{H}_2$  adsorbing on the nickel surface and keep the high surface activity so that sample c has the highest hydrogen storage capacity in the PCT measurement.

**TABLE 2: Catalytic Effect on the Acetone Hydrogenation Conversion and Selectivity at 473 K over (a) 1% Pd/Silica, (b) 40% Ni/Silica Hollow Spheres, and (c) 1% Pd, 40% Ni/Silica Hollow Sphere Catalysts (Acetone = 7.5 mL h<sup>-1</sup>; Acetone:H<sub>2</sub> (molar) = 1:4; Weight of the Catalyst = 0.30 g)**

catalyst	conversion (%)			selectivity at 473 K (%)				
	373 K	423 K	473 K	2-P	IBMK	IBMC	DIPE	others
a	5.2	9.6	29.6	99.0	0	0	0	1.0
b	78	75	70	82.7	13.8	3.0	0	0.5
c	77	68	71	75.6	5.4	1.5	8.2	9.3

The catalytic activity of this material and the function as a carrier for noble metal catalysts were evaluated by the acetone hydrogenation reaction at 373, 423, and 473 K.<sup>16</sup> The reactions were carried out at atmospheric pressure in a fixed-bed reactor. The main products of 2-propanol (2-P), isobutyl methyl ketone (IBMK), and isobutyl methyl carbinol (IBMC) were collected at 0 °C and analyzed by GC-MS. At 473 K, all the catalysts showed a certain activity at this temperature; therefore the selectivities are listed and compared in Table 2. With a small amount of catalyst, a minor H<sub>2</sub>/acetone ratio, and high velocity of acetone, this material exhibits relatively high conversion and good selectivity. It was also found that some diisopropyl ether (DIPE) appeared in the products with 1% Pd and 40% Ni/SiO<sub>2</sub> as the catalyst, but it was not detected in other products.

## Conclusions

The above studies illustrate a route for synthesizing nickel–silica composite hollow nanospheres. The nanospheres are 650 nm in outer diameter, with a thickness of 40 nm. The shells were found to be composed of nickel nanoparticles with an average size of 15 nm. The as-prepared hollow nanospheres exhibit high catalytic activity and good selectivity in acetone hydrogenation reaction, showing potential applications as nanocatalysts in the future. It is expected that further work could lead to the as-prepared nickel–silica composite hollow nanospheres being used in industry.

**Acknowledgment.** This work was supported by the National Natural Science Foundation of China (Grants 20125103 and 90206034).

## References and Notes

- (1) Polman, A.; Wiltzius, P. *MRS Bull.* **2001**, 26, 608.
- (2) Jiang, P.; Cizeron, J.; Bertone, J. F.; Colvin, V. L. *J. Am. Chem. Soc.* **1999**, 121, 7957.
- (3) Gau, H.; Herminghaus, S.; Lenz, P.; Lipowsky, R. *Science* **1999**, 283, 46.
- (4) Caruso, F.; Caruso, R. A.; Mohwald, H. *Science* **1998**, 282, 1111.
- (5) Hu, Y.; Chen, J. F.; Chen, W. M. Lin, X. H.; Li, X. L. *Adv. Mater.* **2003**, 15, 726.
- (6) Dong, A. G.; Ren, N.; Tang, Y.; Wang, Y. J.; Zhang, Y. H.; Hua, W. M.; Gao, Z. *J. Am. Chem. Soc.* **2003**, 125, 4976.
- (7) Jiang, P.; Bertone, J. F.; Colvin, V. L. *Science* **2001**, 291, 453.
- (8) Kulinowski, K. M.; Jiang, P.; Vaswani, H.; Colvin, V. L. *Adv. Mater.* **2000**, 12, 833.
- (9) Yan, H. W.; Blanford, C. F.; Holland, B. T.; Parent, M.; Smyrl, W. H.; Stein, A. *Adv. Mater.* **1999**, 11, 1003.
- (10) Rolison, D. R. *Science* **2003**, 299, 1698.
- (11) Takahashi, R.; Sato, S.; Sodesawa, T.; Kato, M.; Takenaka, S.; Yoshida, S. *J. Catal.* **2001**, 204, 259.
- (12) James, T. R.; Regis, J. D. *J. Catal.* **1978**, 54, 207.
- (13) Stöber, W.; Fink, A.; Bohn, E. *J. Colloid Interface Sci.* **1968**, 26, 62.
- (14) Chen, J.; Li, S. L.; Tao, Z. L.; Shen, Y. T.; Cui, C. X. *J. Am. Chem. Soc.* **2003**, 125, 5284.
- (15) Shim, J.; Lee, H. K. *Mater. Chem. Phys.* **2001**, 69, 72.
- (16) Narayanan, S.; Unnikrishnan, R. *J. Chem. Soc., Faraday Trans.* **1998**, 94, 1123.